

Sonochemical Degradation Rates of Volatile Solutes

A. J. Colussi,* Hui-Ming Hung, and Michael R. Hoffmann*

Environmental Engineering Science, California Institute of Technology, Pasadena, California 91125

Received: October 29, 1998; In Final Form: February 3, 1999

We report degradation rates of chlorinated methanes, ethanes, and ethenes—spanning the range of Henry's law constants $0.9 \leq H/(\text{atm M}^{-1}) \leq 24.5$ —in water solutions sonicated at $f = 205, 358, 618,$ and 1078 kHz. First-order degradation rate constants, k_{-X} , vary as $k_{-X} \sim H_X^{0.30 \pm 0.03}$ at all frequencies, change with f by less than a factor of 2 in this range, and peak at about 600 kHz for all species. We show that experimental rates are consistent with (1) complete decomposition of the solute contained in collapsing bubbles, (2) about 15% ultrasound power efficiency for transient cavitation, and (3) a rather flat $N(R_0) \propto R_0^n$, $n \sim 0$, initial radius bubble distribution under continuous sonication. The solute content of collapsing bubbles is composed of the equilibrated vapor at R_0 , plus the amount incorporated by diffusion from the surrounding solution during the acoustically driven expansion from R_0 to R_{max} , the maximum radius attained prior to collapse. The finding that k_{-X} 's decline above 600 kHz is ascribed to the fact that increasingly smaller bubbles collapse at rates reaching a limiting value at sufficiently high frequencies.

Introduction

Ultrasound induces chemical reactions via acoustic cavitation.^{1–6} This phenomenon entails the sudden collapse of microbubbles of critical size generated by expansion of preexisting nuclei during the rarefaction cycle of acoustic waves. Although the chemical effects of ultrasound have been intensively investigated, the complex series of events preceding and following cavitation still defies a coherent description in terms of fundamental physical and chemical processes.⁷ From a practical point of view it would be useful, for example, to estimate the energy efficiency of sonochemical action under given conditions and, ultimately, to improve it. This consideration is particularly relevant to the possible use of ultrasonic degradation of persistent water contaminants in aquifers and potable water supplies.⁸ In this context it is of interest to understand the physical basis of the dependence of sonochemical rates on molecular and acoustical field parameters.⁷

In this paper, we report experimental degradation rates for a series of chlorinated hydrocarbons—a pervasive class of water pollutants—as a function of ultrasound frequency, in an attempt to provide a stringent test of current sonochemical models and gain new insights into the mechanism of sonication. Crucial to this analysis is the realization that most organic vapors fully decompose under the extreme conditions prevalent in collapsing bubbles.⁷ The discussion leads us to deal with several fundamental issues such as the dynamics of bubble expansion and collapse, the extent of mass transfer across the bubble surface prior to collapse, and the distribution of bubble sizes in liquids continuously exposed to ultrasound.^{5b,6a,9,10} As it emerges, sonochemical degradation rates of volatile solutes can be actually estimated within experimental error from generally available information.

Experimental Section

Sonifications were performed on Ar-purged, aqueous solutions ($V = 605$ mL) contained in a covered, jacketed cylindrical reactor coupled to an ultrasound generator (Allied ELAC Nautik)

through an emitting flange ($A = 23.6$ cm²). The actual ultrasound power Π delivered to the reactor was determined by in-situ calorimetry. The reaction temperature was maintained at 283 K throughout by means of a refrigerated circulating bath (Haake A80). In the case of CH_2Cl_2 , CHCl_3 , and CCl_4 solutions, sample aliquots (1 mL) were withdrawn at given intervals and extracted with 0.5 mL of pentane in capped vials. The 0.5 μL aliquots of the pentane extracts were analyzed with a HP 5880A gas chromatograph (HP-5 column) operated in the splitless mode and equipped with electron capture detector. The analysis of other organic products was carried out with a HP 7694 headspace sampler injector in tandem with a HP 5890 Series II GC-FID gas chromatograph equipped with a HP-624 capillary column (30 m \times 0.32 mm \times 1.8 μm). Commercial chlorinated organic compounds: CCl_4 (99.9%, J. T. Baker reagent), CHCl_3 (LC grade), CH_2Cl_2 (EM Science HPLC grade), C_2Cl_4 (99.9%, Sigma-Aldrich), C_2Cl_6 , (98%, Aldrich), CH_3CCl_3 (98%, Aldrich), and $\text{CH}_2\text{ClCHCl}_2$ (98%, Aldrich) were used without further purification. Aqueous solutions were prepared with water purified with a MilliQ UV Plus system (18.2 m Ω cm resistivity).

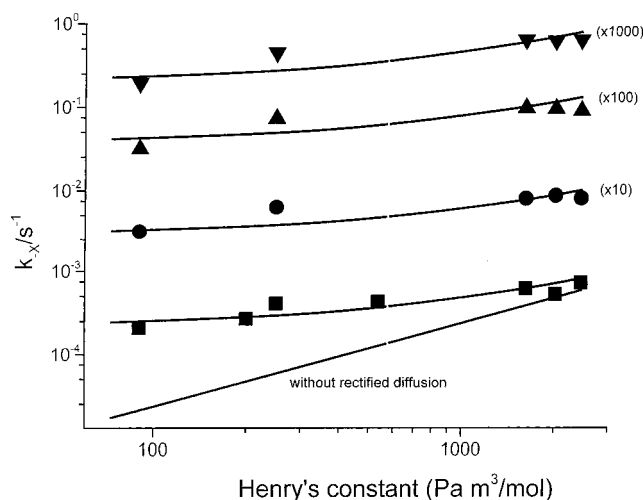
Results and Discussion

Experimental Results. Experiments were routinely performed on solutions (initial concentrations for CH_2Cl_2 , CHCl_3 , and CCl_4 were about 0.15 mM, and ca. 1 μM for the other compounds) sonicated at $\Pi = 50$ W. All solutes decay with first-order kinetics over three half-lives under present experimental conditions. Decay rate constants k_{-X} (s⁻¹) measured for the different solutes at $f = 205, 358, 618,$ and 1078 kHz as function of the corresponding Henry's constants H_X are shown in Table 1 and Figure 1. The nonlinear k_{-X} vs H_X^m dependences found over a 25-fold variation of H values at constant f are conveniently displayed in a scaled log–log plot. Linear regressions yield a mean $m = 0.33 \pm 0.03$ value at the four frequencies. Rate constants are not very sensitive to, but increase with, f up to ca. 600 kHz and then decline.

Decomposition Rates of Volatile Solutes in Cavitated Liquids. Microbubbles present in media steadily exposed to

TABLE 1: Sonochemical Degradation Rate Constants ($\times 10^{-4} \text{ s}^{-1}$) at Different Frequencies and Solubility Parameters for Various Chlorocarbons

species	205 kHz	358 kHz	618 kHz	1078 kHz	Henry's constants ^a H (Pa m ³ mol ⁻¹)
CCl ₄	7.3	8.2	9.2	6.5	2454
CCl ₃ CH ₃	5.4	8.8	9.7	6.3	2025
C ₂ Cl ₄	6.2	8.1	9.9	6.5	1621
CHCl ₃	4.7				537
C ₂ Cl ₆	4.1	6.3	7.3	4.5	250
CH ₂ Cl ₂	2.7				200
CCl ₂ HCClH ₂	2.1	3.2	3.2	1.9	90

^a Taken from ref 13.**Figure 1.** First-order rate constants k_x for the decomposition of volatile solutes. Experimental data from Table 1: (■) 205 kHz; (●) $\times 10$, 358 kHz; (▲) $\times 100$, 618 kHz; (▼) $\times 1000$, 1078 kHz. Solid lines calculated with eq 11 (see text). The straight line for the 205 kHz data was calculated by neglecting the ΔN_m term in eq 10.

ultrasound can either: (1) undergo periodic size oscillations, (2) expand during the rarefaction cycle of acoustic waves and then collapse violently, (3) slowly dissolve, or (4) escape from the liquid due to the combined effects of mass convection and buoyancy.⁷ The relative probabilities of the four processes are a function of bubble size and applied power. For example, bubbles smaller than the Blake radius R_B (μm):

$$R_B = \frac{0.77\sigma}{P_A - P_H} \quad (1)$$

will dissolve;^{4a} P_A is the acoustic pressure amplitude, P_H is the hydrostatic pressure, and $\sigma = 0.072 \text{ N m}^{-1}$ is the surface tension of water at room temperature. Under present conditions, $I_A = \Pi/A = 2.12 \text{ W cm}^{-2}$, $P_A = (2\rho c I_A)^{1/2} = 2.5 \text{ atm}$ ($\rho = 1000 \text{ kg m}^{-3}$ is water density and $c = 1500 \text{ m s}^{-1}$ is the speed of sound in water), $P_H = 1 \text{ atm}$ ($1 \text{ atm} = 10^5 \text{ Pa}$), we get minimum bubble sizes of about $R_B > 0.36 \mu\text{m}$.^{4a} On the other hand, very large bubbles will move upwardly under buoyancy forces and eventually escape from the liquid. It can be shown that bubbles larger than R_E

$$R_E = \sqrt{\frac{9\eta\nu_b}{2\rho g}} \quad (2)$$

where $\eta = 8.9 \times 10^{-4} \text{ kg m}^{-1} \text{ s}^{-1}$ is the water viscosity and $g = 9.8 \text{ m s}^{-2}$, will rise faster than ν_b . The stationary density of bubbles expelled by buoyancy from a stirred medium at speeds larger than, e.g., $\nu_b = 0.1 \text{ cm s}^{-1}$ will be small under mild

insonation. Hence, we will assume that $R_E \leq 30 \mu\text{m}$, which is more than twice as large as resonance radii under the present conditions.^{4a}

The bubble population in a liquid under continuous sonication is actually maintained by a cycle involving bubble expansion, collapse, and fragmentation stages.^{6,7} Near the end of collapse, the radial acceleration of the bubble shell vanishes and its motion becomes unstable.^{6b} Spherical bubbles are easily distorted and break up, dispersing their contents into the solution. The resulting fragments provide the nuclei for the development of new bubbles. If all fragment sizes were produced with the same probability, as would be expected for a mechanism of random bubble fragmentation, and considering that the coalescence of any but the smallest fragments may be slower than reexpansion in an intense sonic field, a steady-state regime would be characterized by a bubble size distribution function, $dN_o/dR_o = AR_o^n$, with $n \sim 0$. This dependence must be contrasted with the equilibrium distribution in quiescent liquids, for which $n = -3$ or -4 applies.^{6a,9,10}

Besides dynamic restrictions, energetic considerations may limit the maximum bubble number density N_B in a sonicated liquid. Restrictions arise from the fact that the surface energy density E_S associated with the bubble cloud cannot exceed the energy density $E_D = I_A/c$ ($E_D = 14.1 \mu\text{J cm}^{-3}$ in present experiments) of the sonic field. In terms of the average bubble area $\langle S_B \rangle$

$$\langle S_B \rangle = \frac{4\pi \int_{R_B}^{R_E} R_o^{2+n} dR_o}{\int_{R_B}^{R_E} R_o^n dR_o} \quad (3)$$

the surface energy density is given by $E_S = N_B \sigma \langle S_B \rangle$. Therefore, the condition $E_S = \beta E_D$, with $\beta \leq 1$, links n and N_B . The bubble volume fraction F_B —an experimentally accessible parameter related to the effective mass density of a sonicated liquid—that could be sustained in sonochemical experiments can be evaluated from the expression $F_B = N_B \langle V_B \rangle$, where $\langle V_B \rangle$ is the average bubble volume. The latter can be calculated once n is known. There is evidence that F_B generally increases with E_D .¹⁰

It has been shown that the maximum radius a bubble can attain by acoustic expansion prior to cavitating collapse can be estimated from^{4a}

$$R_{\max} \approx (3000/f)(P_A - P_H)(P_A)^{-0.5} [1 + 0.67(P_A - P_H)]^{0.33} \quad (4)$$

or $R_{\max} (\mu\text{m}) = 3589/f$ (kHz) under present conditions. However, not all bubbles can grow to R_{\max} and undergo violent collapses because of the existence of a dynamic threshold: only bubbles with initial radii $R_o \leq R_{\max}/3$ can reach R_{\max} .^{5a} Thus, the bubble subpopulation $\{R_o; R_B \leq R_o \leq R_{\max}/3\}$ that is actually able to undergo cavitation and lead to chemical effects becomes increasingly sparser at higher frequencies (cf. the $R_{\max} \propto 1/f$ dependence in eq 4). Therefore, the density of bubbles that can potentially undergo transient cavitation $N_{B,CAV}$:

$$N_{B,CAV} = N_B \frac{\int_{R_B}^{R_{\max}/3} R_o^n dR_o}{\int_{R_B}^{R_E} R_o^n dR_o} \quad (5)$$

is necessarily smaller than N_B . On the other hand, the maximum rate r_{CAV} (bubbles $\text{cm}^3 \text{ s}^{-1}$) at which bubbles can be expanded

to R_{\max} also depends on ultrasound power Π according to⁷

$$r_{\text{CAV}} = (\Pi/V)/\epsilon_B \quad (6)$$

where ϵ_B is the energy required to expand potentially cavitating bubbles (i.e., those having $R_o \leq R_{\max}/3$):^{5a,7}

$$\epsilon_B = (4\pi/3)(P_A + P_H)(R_{\max}^3 - R_o^3) + 4\pi\sigma(R_{\max}^2 - R_o^2) \approx (4\pi/3)(P_A + P_H)R_{\max}^3 + 4\pi\sigma R_{\max}^2 \quad (7)$$

As a consequence, the average frequency k_E at which bubbles are excited, k_E (s^{-1}) = $r_{\text{CAV}}/N_{\text{B,CAV}}$, is a strongly increasing function of f , because (1) $r_{\text{CAV}} \propto (1/\epsilon_B) \propto (1/R_{\max}^3) \propto f^3$ (cf. eqs 3, 6, and 7) and (2) $N_{\text{B,CAV}}$ decreases with f on account of the narrowing of the subpopulation of cavitating bubbles (cf. the upper integration limit in the numerator of eq 5). Notice that k_E cannot obviously exceed f and, therefore, the efficiency of cavitation becomes limited by this factor at high frequencies.

Recent calculations on the fate of volatile species in cavitating bubbles indicate that they are completely decomposed at the high temperatures attained at the end of collapse.^{7,11} Hence, solute decomposition rates r_{-X} can be evaluated as the product of the rate of generation of cavitating bubbles r_{CAV} (eq 6), times the total amount of solute N_T contained in such bubbles. The total number of solute molecules consists of those present within initial nuclei, N_m , plus those admitted during the expansion stage ΔN_m . Assuming liquid–vapor equilibrium, the former is given by⁷

$$N_m = \frac{4\pi R_o^3 H C_\infty}{3RT} \quad (8)$$

where H is the solute Henry's constant, C_∞ is the solute bulk concentration, and R is the gas constant. During expansion, an additional mass of solute enters from the initially saturated solution into the rarefied bubble. We evaluated ΔN_m using the high-frequency form of the first-order approximation to dynamic rectified diffusion derived by Eller and Flynn:^{5a,12}

$$\Delta N_m = C_{R_o} \left(\frac{C_\infty}{C_{R_o}} - \frac{\langle (R/R_o) \rangle}{\langle (R/R_o)^4 \rangle} \right) \left[8\sqrt{\pi D t \langle (R/R_o)^4 \rangle} R_o^2 + 4\pi D t R_o \langle (R/R_o) \rangle \right] \quad (9)$$

where $C_{R_o} = C_\infty [1 + 2\sigma/(P_H R_o)]$ and $D \sim 2 \times 10^{-5} \text{ cm}^2 \text{ s}^{-1}$ is the assumed common value of solute diffusion coefficients in water at 300 K. Lower, approximate bounds to the required time averages of R were estimated for bubbles expanding at constant velocity, i.e., $\langle (R/R_o) \rangle \sim 1 + 0.5 [(R_{\max}/R_o) - 1]$, $\langle (R/R_o)^4 \rangle \sim (1/5)[(R_{\max}/R_o)^5 - 1]/[(R_{\max}/R_o) - 1]$. Therefore, first-order decay rate constants k_{-X} for solute decomposition in bubbles of radius R_o can be calculated from

$$k_{-X} = \varphi r_{\text{CAV}}(N_m + \Delta N_m)/C_\infty \quad (10)$$

where φ is the energy efficiency of cavitation, i.e., the fraction of ultrasound energy actually utilized in bubble cavitation. It is assumed that φ is independent of f . Average values $\langle k_{-X} \rangle$, i.e., those to be compared with experimental data, involve averaging k_{-X} over the bubble size distribution:

$$\langle k_{-X} \rangle = \frac{\int_{R_B}^{R_{\max}/3} k_{-X} R_o^n dR_o}{\int_{R_B}^{R_{\max}/3} R_o^n dR_o} \quad (11)$$

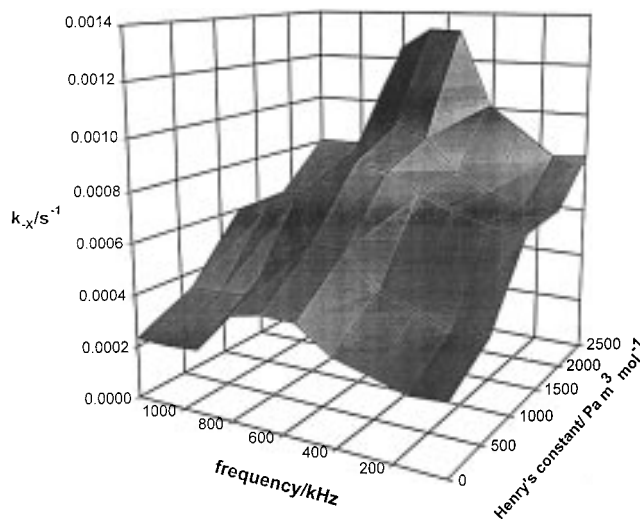


Figure 2. The landscape of k_{-X} as a function of f and H , calculated from eq 11 (see text).

Trial fits of $\langle k_{-X} \rangle$, calculated by means of eq 11 at $f = 205, 358, 618,$ and 1078 kHz, to the experimental data for the chlorocarbons of Table 1, were performed using n (the exponent in R_o^n of the bubble radii distribution), φ (the energy efficiency of transient cavitation), and β (the fraction of the acoustic field energy stored as surface energy of the bubble cloud) as adjustable parameters. The results of calculations are shown in Figures 1 and 2. Typical sets of parameters reproducing experimental data are, e.g., $\{n = 0.5, \varphi = 0.15, \beta = 1\}$ and $\{n = 0, \varphi = 0.15, \beta = 0.1\}$. The latter set implies a volume fraction of $F_B \sim 1 \times 10^{-4}$, i.e., close to the upper limit of the range suggested for water in cavitation tubes.¹⁰ We found that the onset of the k_{-X} falloff as a function of f remains at about 600 kHz largely through the interplay of n and β . The nonlinear k_{-X} vs H dependences at all frequencies, as well as the peak efficiencies at $f \sim 600$ kHz for all substrates are well accounted for by the model. We also found that in order to reach peak efficiencies at ~ 600 kHz with $n \leq 0$ it is necessary to invoke much larger R_E values. For example, $n = -1$ requires $R_E \geq 250 \mu\text{m}$, which is considered implausible. By setting $R_E = 30 \mu\text{m}$, calculations with $n = -3$ result in a monotonic, 4-fold increase of $\langle k_{-X} \rangle$ between 205 and 1078 kHz. The $n = -3$ equilibrium distribution is so slanted toward small sizes that nearly the same bubble pool is excited at all frequencies, despite the fact that the condition $R_o \leq R_{\max}/3$ would allow for transient cavitation of larger bubbles at lower frequencies.

To summarize, the physical reasons underlying the observed behaviors are related to the fact that degradation rates are actually proportional to the density of bubbles excited per unit time—which increases with frequency as f^3 because much less work is required to expand bubbles to smaller $R_{\max} \sim 1/f$ values—times the amount of solute accumulated within bubbles at the time of their collapse. Such an amount is generally dominated by a leading term ΔN_m (the amount of solute incorporated into the bubble during expansion, eq 9) that roughly decreases as $\sim 1/f^2$. The breakdown of the expected $\langle k_{-X} \rangle \propto f$ dependence at high frequencies is a consequence of the fact that the intermittence at which individual bubbles are excited cannot exceed f . As a result, the $1/f^2$ dependence gradually takes over with the consequent slow down of decomposition rates. The nonlinear k_{-X} vs H_X dependence directly reveals that rate constants are not solely determined by equilibrium parameters. Rectified diffusion contributes significantly to the composition

of the bubble vapor prior to collapse, particularly for the less volatile substrates. Further work is underway.

Acknowledgment. Financial support for this research was provided by the U.S. Department of Energy (DOE 1 963772 402).

References and Notes

- (1) Suslick, K. J., Ed. *Ultrasound, Its Chemical, Physical and Biological Effects*; VCH: Weinheim, Germany, 1988.
- (2) Margulis, M. A., Ed. *Sonochemistry and Cavitation*; Gordon and Breach: Newark, NJ, 1995.
- (3) Henglein, A. *Ultrasonics* **1987**, 25, 6.
- (4) (a) Mason, T. J.; Lorimer, J. P. *Sonochemistry. Theory, Applications and Uses of Ultrasound in Chemistry*; Wiley: New York, 1988; Chapter 2. (b) Mason, T. J., Ed. *Advances in Sonochemistry*; JAI Press: New York, 1990–1994; Vols. 1–3.
- (5) (a) Leighton, T. G. *The Acoustic Bubble*; Academic Press: London, 1994; Chapter 4, section 4.4.3. (b) Leighton, T. G. *Ultrason. Sonochem.* **1995**, 2, S123.
- (6) (a) Brennen, C. E. *Cavitation and Bubble Dynamics*; Oxford University Press: New York, 1995; section 1.11. (b) *Ibid.*, section 2.12.
- (7) Colussi, A. J.; Weavers, L. K.; Hoffmann, M. R. *J. Phys. Chem. A* **1998**, 102, 6927.
- (8) (a) Graham, J. L.; Hall, D. L.; Dellinger, B. *Environ. Sci. Technol.* **1986**, 20, 703. (b) Hua, I.; Hoffmann, M. R. *Environ. Sci. Technol.* **1997**, 31, 2237.
- (9) Gavrilov, L. R. in *Physical Principles of Ultrasonic Technology*; Plenum Press: New York, 1973; Vol 2, Part VI.
- (10) Gavrilov, L. R. *Sov. Phys.-Acoust.* **1970**, 15, 285.
- (11) Westley, F.; Frizzell, D. H.; Herron, J. T.; Hampson, R. F.; Mallard, W. G. (a) NIST Chemical Kinetics Database 17, Version 5.0; National Institute of Standards and Technology: Gaithersburg, MD, 1993. (b) Baulch, D. L.; Cobos, C. J.; Frank, P.; Hayman, G.; Just, Th.; Murrells, T.; Pilling, M. J.; Troe, J.; Walker, R. W.; Warnatz, J. *J. Phys. Chem. Ref. Data* **1994**, 23, 847.
- (12) Eller, A. I.; Flynn, H. G. *J. Acoust. Soc. Am.* **1965**, 37, 493.
- (13) Mackay, D.; Shiu, W. Y.; Ma, K. C. *Illustrated Handbook of Physical-Chemical Properties and Environmental Fate of Organic Chemicals*; Lewis Publishers: Boca Raton, FL, 1993; Vol. III.